EL NIÑO SOUTHERN OSCILLATION (ENSO)-INDUCED PM_{10} VARIABILITY IN MINING AREAS WITHIN THE 2014–2017 PERIOD

HELI A. ARREGOCÉS[1,2], ROBERTO ROJANO[1] & GLORIA RESTREPO[2]
[1]Grupo de Investigación GISA, Facultad de Ingeniería, Universidad de La Guajira, Colombia
[2]Grupo Procesos Fisicoquímicos Aplicados, Facultad de Ingeniería,
Universidad de Antioquia SIU/UdeA, Colombia

ABSTRACT

Given that El Niño Southern Oscillation (ENSO) phenomena had significant environmental impacts in 2015–2016, this study presents an exploratory analysis of PM_{10} variability in open-pit mining areas in northern Colombia. PM_{10} and meteorological variables were measured at three locations, and analyses were performed. The results obtained showed that ENSO plays an important role in the temporal distribution of daily precipitation, and its occurrence resulted in an 8.3% decrease in annual average precipitation within the period of February 2015–May 2016. However, it had no significant effect on temperature, relative humidity, and wind speed within the study period. Further, the annual mean PM_{10} concentration corresponding to all the stations considered in this study between 2014 and 2017 was 34 $\mu g/m^3$ (95% CI, 33–35 $\mu g/m^3$), and the standard deviation was ± 11.59 $\mu g/m^3$. The individual arithmetic means of PM_{10} concentrations at the different stations were 1.11–2.07 times the WHO air quality guidelines for PM_{10} but did not exceed the maximum level permissible specified by the Colombian norm. Furthermore, the average PM_{10} concentrations in all the samples corresponding to the El Niño classified Oceanic Niño Index (ONI) phase (37.14 $\mu g/m^3$; CI95% 36.06–38.22 $\mu g/m^3$) were numerically higher than those corresponding to the neutral classified ONI phase (32.54 $\mu g/m^3$; CI95% 31.82–33.27 $\mu g/m^3$), and the correlation coefficients between PM_{10} and meteorological parameters were found to be relatively low.

Keywords: PM_{10}, ENSO, ONI, variability, air quality.

1 INTRODUCTION

The El Niño Southern Oscillation (ENSO) is an atmosphere/ocean phenomenon of significance owing to its global effects and multiple interrelations. ENSO events are associated with economic losses due to different conditions resulting from the teleconnections that exist between them and other factors such as climate and public health in different areas. Additionally, ENSO is considered to be the most important climate cycle that is usually associated with the interannual variability climate, with the possibility of engendering extreme weather events, such as heavy rainfall, droughts, and storms [1]. Studies on the temporal and spatial behavior of $PM_{2.5}$ and PM_{10} have shown that their distribution strongly depends on meteorological variables [2], [3]. Consequently, the effects of meteorological variables on the formation and deposition of atmospheric particles are well established [4]–[6].

The ENSO phenomenon brings about dry conditions in the north and northeast of South America, and consequently opposite conditions in the southeast and southwest regions. This behavior is due to the anomalies that are associated with the Walker circulation and the Hadley cells on both sides of the equator [7]. These interannual climatic variations that cause precipitation anomalies have been reported in several studies [8]–[10].

Further, from a public health perspective, ENSO events are associated with changes in marine ecosystems and the spread of bacterial diseases, which are increasingly propagated owing to the local geographical conditions [11]. Similarly, some epidemiological studies on

WIT Transactions on Ecology and the Environment, Vol 252, © 2021 WIT Press
www.witpress.com, ISSN 1743-3541 (on-line)
doi:10.2495/AIR210191

air pollution have incorporated the correlation between meteorological variables and pollutant concentration levels [12], and several studies have been conducted to clarify how El Niño variability brings about climate responses owing to the patterns of the teleconnections that are associated with other factors. The results of these studies have provided evidence of the influence of ENSO on the variability of the concentration of particulate materials with sizes below 10 μm (PM_{10}) [13], [14]. Furthermore, several studies have been conducted in this regard, focusing on precipitation frequency levels, which significantly influence the transport and dispersion of PM_{10}. Specifically, Singh and Palazoglu [15], [16] studied the effects of ENSO events on particulate matter in six regions in the United States and revealed that such effects are detectable in terms of the seasonal and annual variability of air pollution episodes.

Therefore, given the occurrence of the El Niño phenomenon in northern South America, it can affect local-scale phenomena, particularly the concentrations of pollutants and particulate matter. However, its effects on PM_{10} concentrations in Colombia have not been previously investigated. Therefore, this study focuses on the El Cerrejón mine, which emits some of the highest levels of PM in northern Colombia, with primary aims to (1) statistically analyze the spatiotemporal behavior of PM_{10} concentrations and meteorological data in this mine area and (2) analyze the relationships between PM_{10} levels and ENSO. The remainder of this paper is organized as follows: Section 2 describes the data and methodology used, Section 3 provides the results and discussions considering existing literature, and Section 4 concludes the paper.

2 MATERIALS AND METHODS

The open-pit coal mine and the area affected by the related mining activities are located in northern Colombia (11° 5 N, 72° 40 W). East of this area is the Sierra Nevada de Santa Marta, and in the west are the Perijá Mountains, which lie along the Colombian border with Venezuela. This area includes three municipalities (Albania, Hatonuevo, and Barrancas), and has a total population of 59,089 inhabitants of which 34% are indigenous people. Fig. 1 shows the map of this mining region, with the PM_{10} sampling stations, Barrancas (BR), Las Casitas (LC), Patilla (PT), Provincial (PV), and Sol y sombra (SS) indicated. The figure also shows the locations of the mining emission sources, i.e., the La Puente, Tabaco, Patilla, Comunero, 100, and Oreganal pits.

2.1 Meteorological data

Meteorological measurements corresponding to the 2014–2017 period included hourly mean temperature (T, °C), wind speed (WS, m/s), wind direction (WD, degrees), relative humidity (RH, %), and precipitation (Pp, mm). The data were obtained from the stations with meteorological sensors, i.e., PV, BR, and LC, which are representative of the six main exploitation areas from north to south, i.e., La Puente Pit (LPUp), Tabaco pit (TABp), Patilla pit (PATp), Comunero pit (COMp), 100 pit (100p), and Oreganal pit (OREp). The daily averages of each variable were calculated from the hourly data based on the availability of valid measurements at least 75% each day. The daily averages of WD were calculated using the air quality tool of R-Studio software version 3.6.3, OpenAir [17].

2.2 Monitoring of PM_{10} data

PM_{10} data corresponding to the 2014–2017 period were collected. This period was chosen because it includes PM_{10} data corresponding to one year before and one year after the

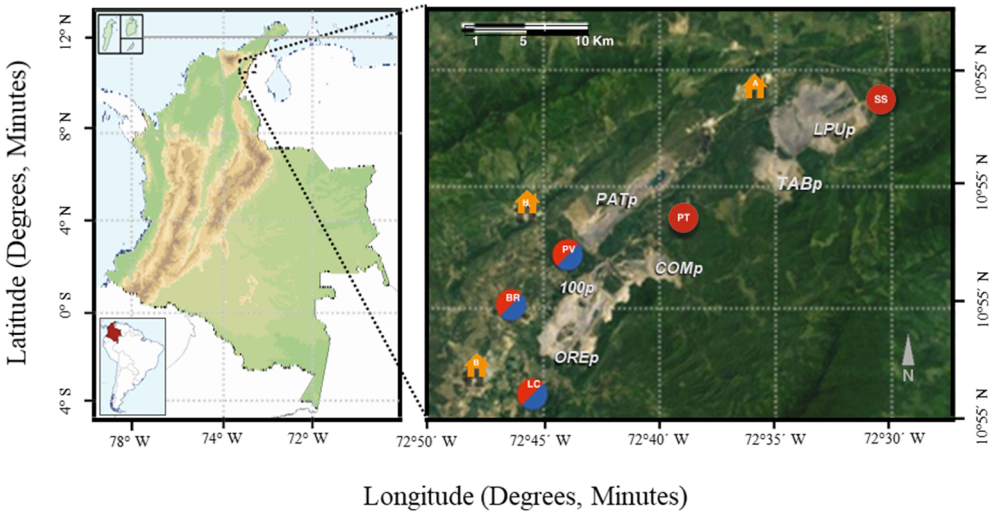

Figure 1: Geographical location of study area showing the PM_{10} sampling stations from north to south: SS (Sol y sombra), PT (Patilla), PV (Provincial), BR (Barrancas), and LC (Las Casitas); and the nearby municipalities, Albania (A), Hatonuevo (H), and Barrancas (B). The extraction pits are also shown. Left panel: Modified from Mapa de Colombia (orografía).svg Wikipedia, https://goo.gl/; Right panel: Google earth v7.1.5.1557, 2016–03–02, DigitalGlobe 2016. http://www.earth.google.com.

occurrence of the 2015–2016 El Niño event. Specifically, particulate matter samples were collected using a high-volume sampler (Hi-Vol TE- 6,070) obtained from Tisch Environmental Company (Cleves, OH, USA). Thereafter, PM_{10} samples were obtained using Whatman® quartz filters (8 × 10 in.), after which they were processed and analyzed using gravimetric techniques, according to the procedure established in the Code of Federal Regulations (Appendix J to Part 50, PM_{10}) [18]. The filters were conditioned at 35 ± 5% RH and 23 ± 1°C for at least 24 h before weighing using a Sartorius MC 5 Microbalance, packaging, and shipping to Columbia. The process of preparing and weighing the filters was implemented at the Center for Air Resources Engineering and Science, Clarkson University. Table 1 shows the geographical locations of the sampling stations and the variables measured at each station.

PM_{10} samples were obtained every 3 days for 24 h from 3 January 2014 to 28 December 2017. The readings obtained for BR, LC, PT, PV, and SS were 428,444, 322, 440, and 449, respectively. Quality control was performed on the analyzed samples.

2.3 Oceanic Niño Index (ONI) phases classification

El Niño occurrence was estimated using data from the ONI. The ONI data were obtained from the National Oceanic and Atmospheric Administration (NOAA). The values in red corresponded to El Niño, while those in blue corresponded to El Niña [19]. ONI values can be used to identify Pacific surface area anomalies over a moving average of three months

Table 1: Geographical coordinates of the designated sampling sites. The measured variables and the elevations of the sampling sites (above sea level, m) are also shown.

Site name	ID	Latitude (°)	Longitude (°)	Elevation (m)	Variables measured
Sol y Sombra	SS	11° 8′ 37.88″ N	72° 30′ 36.64″ W	117	PM_{10}
Patilla	PT	11° 30′ 00″ N	72° 40′ 15.60″ W	115	PM_{10}
Provincial	PV	11° 1′ 23.12″ N	72° 44′ 5.99″ W	156	PM_{10}, *T*, *Pp*, HR, ws, wd
Barrancas	BR	10° 57′ 34.38″ N	72° 46′ 45.52″ W	150	PM_{10}, *T*, *P*p, HR, ws, wd
Las Casitas	LC	10° 57′ 1.69″ N	72° 44′ 28.23″ W	162	PM_{10}, *T*, *Pp*, HR; ws, wd

(Table 2). The warm (red) and cold (blue) periods are based on a threshold of ±0.5°C. If ONI values above +0.5°C are recorded within five consecutive months, the period is characterized as an El Niño period. Conversely, when the index values are below –0.5°C for the same number of months, the period is characterized as La Niña. In this study, the El Niño intensity was classified as weak, moderate, and strong when the ONI values were in the ranges 0.5–0.9, 1–1.4, and > 1.5, respectively.

Table 2: El Niño intensity within the 1990–2017 period based on Oceanic Niño Index (ONI) values and classifications from 1990 to 2017. (Data adapted from the NOAA.)

Year	DJF	JFM	FMA	MAM	AMJ	MJJ	JJA	JAS	ASO	SON	OND	NDJ
2014	–0.4	–0.5	–0.3	0	0.2	0.2	0	0.1	0.2	**0.5**	**0.6**	**0.7**
2015	**0.5**	**0.5**	**0.5**	**0.7**	**0.9**	**1.2**	**1.5**	**1.9**	**2.2**	**2.4**	**2.6**	**2.6**
2016	**2.5**	**2.1**	**1.6**	**0.9**	0.4	–0.1	–0.4	**–1**	**–0.6**	**–0.7**	**–0.7**	**–0.6**
2017	–0.3	–0.2	0.1	0.2	0.3	0.3	0.1	–0.1	–0.4	**–0.7**	**–0.8**	**–1**

3 RESULTS AND DISCUSSION

3.1 Meteorological conditions during ENSO

Fig. 2 shows the monthly variability of the meteorological parameters considered in this study. The annual average temperature was 29.5°C (percentile 25%, Q1 = 28.1°C; percentile 25%, Q3 = 30.7°C), and the annual average RH was 65% (percentile 25%, Q1 = 59%; percentile 25%, Q3 = 70%). Further, the average speed of the observed predominant ENE winds (frequencies ~ 30%) was 2.90 m/s (percentile 25%, Q1 = 2.00 m/s; percentile 25%, Q3 = 3.60 m/s).

ENSO played an important role in the temporal distribution of daily precipitation, bringing about a decrease in precipitation owing to the changes in temperature in the Pacific Ocean. This phenomenon resulted in low precipitation in the Colombian Caribbean zone, with the maximum and minimum precipitation values being 119.20 and 1.10 mm, respectively. The annual historical average of the registered precipitation in this area was 738 mm, with two rainy seasons, the first from February to May (short season) and the second from August to November (long season) [20].

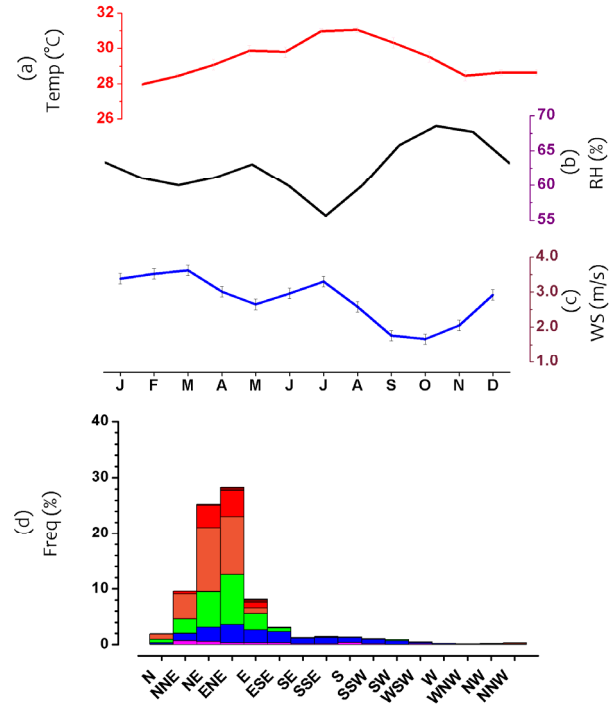

Figure 2: Monthly variability of meteorological parameters. (a) Temperature (°C); (b) Humidity relative (%); (c) Wind speed (ms^{-1}); and (d) Predominant wind direction (Freq, %).

Further, during the study period, an 8.3% decrease in annual average precipitation was observed owing to the occurrence of the ENSO phenomenon. This annual historical average precipitation diminished by 17% during the first rainy season (March–May), and a lower percentage decrease (4%) was observed during the second rainy season (August–November). These decreases are consistent with those reported by Córdoba-Machado et al. [21] and Poveda et al. [22].

To determine the origin of the differences between the stations in the extraction mine area (PV, BR, and LC) with respect to temperature, RH, precipitation, and wind, ANOVA was performed. In general, no significant differences between stations were observed with respect to these parameters ($p > 0.05$). The results showed that the meteorological conditions were uniform throughout the extraction area, including the El Cerrejón area. The temperature varied by 0.25–2.46% per year, with the LC station showing the highest variation level (2.46% per year). These temperature trends were not statistically significant ($p > 0.05$) at all the sites. Further, RH varied between –1.58 and 1.05% per year, with the LC station showing the highest variation level (–1.58% per year). The decreasing RH trend showed statistical significance ($p < 0.05$) at the LC station (–0.98°C/year). WS variation ranged between –5.75 and 2.17% per year, with the LC station showing the highest variation level (–5.75% per year). These WS variation trends were not statistically significant at all the stations, and at the BR station (–5.75% per year) and the PV station

(–1.08% per year), it was decreasing, while at the LC station (2.17% per year), it was increasing.

Pearson correlation analysis was performed to determine the level of correlation between ONI values and the meteorological parameters (T, WS, HR, and Pp) at the different study sites. The analysis showed positive correlations between the ONI values and temperature ($r^2 = 0.16$) and wind speed ($r^2 = 0.18$) at all the stations. Conversely, negative correlations were observed for humidity relative ($r^2 = –0.22$) and precipitation ($r^2 = –0.24$). Further, during the three seasons, the variations of the correlation coefficients between monthly precipitation and the ONI values were less significant during the El Niño period. Furthermore, at the three stations, the correlation coefficients varied in the ranges 0.006–0.012 and 0.158–0.491 in El Niño classified ONI phases (year = 2015) and neutral classified ONI phases, respectively.

3.2 PM_{10} concentrations

The annual mean concentration of PM_{10} for all the sampling stations in the study area between 2012 and 2016 was 34 μg/m^3 (95% CI 33–35 μg/m^3) and the standard deviation was ± 11.59 μg/m^3. In the analysis by season, the highest concentrations were observed at the LC station (41 μg/m^3; CI95% 40–42 μg/m^3), followed by the PV station (38 μg/m^3; CI95% 37–39 μg/m^3), BR station (35 μg/m^3; CI95% 33–36 μg/m^3), PT station (34 μg/m^3; CI95% 32–36 μg/m^3), and SS station (23 μg/m^3; CI95% 22–24 μg/m^3). The individual arithmetic averages at each station did not exceed the maximum permissible level (MLP) specified by the Colombian norm (MLP; daily average of 75 μg/m^3 and annual average of 50 μg/m^3 for PM_{10}). However, they were 1.11–2.07 times the value specified in the WHO air quality guidelines for PM_{10} (annual mean of 20 μg/m^3). Table 3 presents a summary of the statistics corresponding to the different monitoring sites throughout the study period. The site with the highest PM_{10} concentration was the LC station, which is located SW of the mining operation area (downwind), and that with the lowest PM_{10} concentration was the SS station, which is located NE of the mining operation area (upwind).

Table 3: Statistical data corresponding to all the stations within the 2014–2017 period.

Stations	Min	Max	Q_1	Median	Mean	Q_3	IC	Desv. Est.
PT	9.05	103.7	25.2	32.39	35.19	42.2	1.3	13.09
BR	6.65	96.22	24	33.1	34.35	42.1	1.3	14.23
LC	4.77	94.92	29.4	39.59	41.5	50	1.4	16.25
PV	5.95	87.39	28.6	35.99	38.46	46.6	1.3	14.08
SS	4.87	89.98	14.2	21.02	22.28	29.6	1.1	12.64
All	4.77	103.7	23.2	32.4	34.3	43.4	0.6	15.42

The Sen–Theil estimator, which uses the median of the slopes of all the lines connecting pairs of two-dimensional sample points, was used to estimate the time trends for PM_{10} sampling at each station within the 2012–2016 period. Thus, it was observed that PM_{10} showed increasing concentration trends at the PT, BR, and SS stations ($p < 0.01$), with the estimated slopes ranging between 6.2 and 7.7% per year; thus, the high significance observed for the BR and PT sites. Conversely, the LC and PV sites showed no significant trends ($p > 0.1$). Pearson correlation coefficients corresponding to the relationship between PM_{10} concentrations at the different sites were determined. All the values showed

significance at 95% CI, with r ranging between 0.42 and 0.83, indicating a common PM_{10} emission source in the study area.

3.3 PM_{10} concentrations during ENSO

The average concentrations of PM_{10} in all the collected samples corresponding to the years in the El Niño classified ONI phase (37.14 μg/m^3; CI95% 36.06–38.22 μg/m^3) were numerically higher than those of the samples corresponding to the years in the neutral classified ONI phase (32.54 μg/m^3; CI95% 31.82–33.27 μg/m^3). A boxplot was used to illustrate the descriptive statistics of the PM_{10} concentrations in the neutral and El Niño phases (Fig. 3). The range of the values in the upper quartile (Q3) and lower quartile (Q1) for the neutral phase (22.88–43.70 μg/m^3) was lower than that corresponding to the El Niño classified ONI phase (26.32–47.60 μg/m^3). These results indicate that higher observed PM_{10} concentrations are related to the El Niño phenomenon.

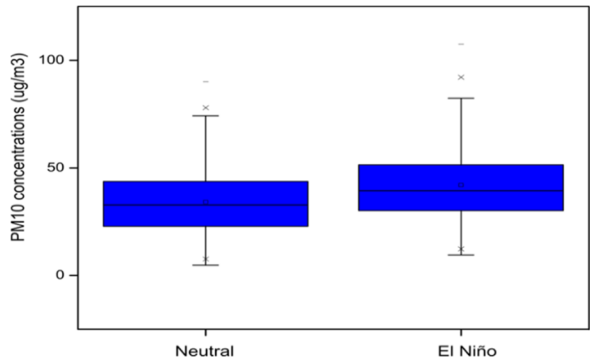

Figure 3: Box plots of daily PM_{10} concentrations for the neutral and El Niño classified ONI phases.

The results corresponding to different sampling sites were compared using ANOVA, which allowed the identification of statistically significant differences ($p < 0.05$) between PM_{10} concentrations in neutral and El Niño phases. The ANOVA results indicated that the difference between the monthly averaged PM_{10} concentrations corresponding to the neutral and El Niño phases were not statistically significant for BR ($p = 0.001$), PT ($p = 0.001$), and SS ($p = 0.036$) stations. However, they were significant for the LC ($p = 0.922$) and PV ($p = 0.330$) stations.

Further, Fig. 4 shows the monthly variation of ONI values between 2014 and 2017 as well as the variation of daily PM_{10} concentrations for all the sampling sites (PT, BR, LC, PV, and SS) for the same period. The highest PM_{10} concentrations were observed between August and December 2015 and January and March 2016. Similarly, a slight increase in PM_{10} concentration was observed between August and December 2015 and January and March 2016, compared with the other years considered in this study. This behavior can be explained considering the observed precipitation patterns. As mentioned in Section 3.1, for 2015, the annual historical average precipitation decreased by 17% during the first rainy season (March–May) and by 4% during the second rainy season (September–November).

Therefore, a higher level of precipitation could bring about a decrease in atmospheric PM_{10} concentrations owing to its scavenging effect.

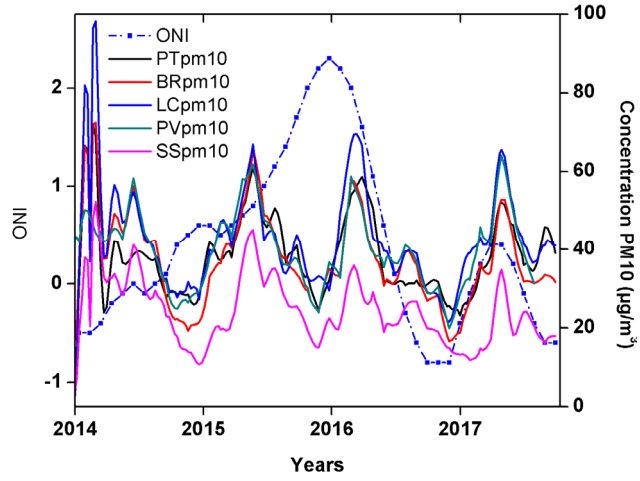

Figure 4: Monthly variation of the Oceanic Niño Index (ONI) and variation of daily PM_{10} concentrations at all the sampling sites between 2014 and 2017.

Pollutant concentration significantly depends on weather conditions, which influence the diffusion, dilution, and accumulation of pollutants [23], [24]. At the stations, where meteorological parameters were measured (i.e., BR, LC, and PV), PM_{10} showed a negative correlation with RH (r ranging from –0.15 to –0.34) and precipitation (r ranging from –0.14 to –0.25). However, at these stations, it showed a positive correlation with temperature (r ranging from 0.10 to 0.36) and wind speed (r ranging from 0.18 to 0.33). Although the correlation coefficients were relatively low, the influence of meteorological variables on the particulate matter concentration remained indisputable [25]. The low correlations may be explained by other factors that were not considered in this study: emissions rates in the mining area, regional biomass burning, and variability of the planetary boundary layer. Meteorological anomalies resulting from ENSO have an impact on PM_{10} concentrations. The most significant relationships can be attributed to precipitation anomalies, vertical temperature variability, and barometric pressure trends. Precipitation anomalies during ENSO fall below normal levels by up to 17%. El Niño effects on precipitation are associated with interactions between the ENSO seasonality, teleconnection patterns, and local climate [26]. Global model reanalysis data indicate that at different geopotential heights, highly significant temperature inversions occurred during ENSO (https://psl.noaa.gov/data/gridded/data.ncep.reanalysis.html). Vertical-scale temperature inversions generate higher levels of stability between atmospheric layers, which influences updrafts and provides less stability to surface air masses, thus creating poor circulation conditions [27]. This study does not consider the impact of emissions on pollution levels and the results do not allow the prediction of pollution events caused by increased local emissions. These values are shaped by the ability to relate the patterns of variability of local meteorological conditions leading to high PM_{10} concentrations, which helps to distinguish air quality conditions driven by anthropogenic activities from those induced by natural phenomena.

4 CONCLUSIONS

The results of this study showed that meteorological parameters, temperature, RH, and WS, did not vary significantly owing to the occurrence of the ENSO phenomenon. Conversely, precipitation varied significantly in this regard. Specifically, average precipitation diminished significantly during the first rainy season (March–May). However, the decrease was not significant during the second rainy season (August–November).

The individual arithmetic averages of PM_{10} concentrations at each station were higher than the value specified by the WHO air quality guidelines for PM_{10} but did not exceed the maximum level permissible specified in the Colombian norm. ENSO affected PM_{10} concentrations in the El Cerrejón mine, primarily owing to changes in precipitation; however, some critical factors cannot be ruled out. For example, contributions from communities located close to the stations. Further, a significant correlation was observed between the ENSO phenomenon and PM_{10} concentrations at stations located downwind of the extraction area, i.e., the LC and PV stations, which are located in towns that are close to the extraction site. However, at stations located in the center and upwind of the extraction area, i.e., the SS, PT, and BR stations, no correlations were observed in this regard.

ACKNOWLEDGEMENTS

The author would like to thank MinCiencias Colombia (Biannual Plan-Excellence Scholarship Program), the University of La Guajira and University of Antioquia.

REFERENCES

[1] Kovats, R.S., Bouma, M.J., Hajat, S., Worrall, E. & Haines, A., El Niño and health. *Lancet*, **362**(9394), pp. 1481–1489, 2003.

[2] Li, L., Wu, A.H., Cheng, I., Chen, J.-C. & Wu, J., Spatiotemporal estimation of historical $PM_{2.5}$ concentrations using PM_{10}, meteorological variables, and spatial effect. *Atmos. Environ.*, **166**, pp. 182–191, 2017.

[3] Tiwari, S. et al., Assessment of $PM_{2.5}$ and PM_{10} over Guwahati in Brahmaputra river valley: Temporal evolution, source apportionment and meteorological dependence. *Atmos. Pollut. Res.,* **8**(1), pp. 13–28, 2017.

[4] Alonso-Blanco, E. et al., Temporal and spatial variability of atmospheric particle number size distributions across Spain. *Atmos. Environ.*, **190**, pp. 146–160, 2018.

[5] André, F., Jonard, M. & Ponette, Q., Influence of meteorological factors and polluting environment on rain chemistry and wet deposition in a rural area near Chimay, Belgium. *Atmos. Environ.*, **41**(7), pp. 1426–1439, 2007.

[6] Zhang, Y. et al., The influence of relative humidity on the heterogeneous oxidation of sulfur dioxide by ozone on calcium carbonate particles. *Sci. Total Environ.,* **633**, pp. 1253–1262, 2018.

[7] Oort, A.H. & Yienger, J.J., Observed interannual variability in the Hadley circulation and its connection to ENSO. *J. Clim*., pp. 2751–2767, 1996.

[8] Cazes Boezio, G., Talento, S. & Pisciottano Jalabert, G.J., Seasonal probability forecasts of Dec.-Jan.-Feb. precipitation in northern Uruguay and Rio Grande do Sul obtained with the coupled forecast system 2 of NOAA and statistical downscaling. *Rev. Bras. Meteorol.*, **27**(4), pp. 377–387, 2012.

[9] Grimm A.M. & Tedeschi, R.G., ENSO and extreme rainfall events in South America. *J. Clim.*, **22**(7), pp. 1589–1609, 2009.

[10] Bernal, G., Ruiz-Ochoa, M. & Beier, E., Variabilidad estacional e interanual océano-Atmósfera en la cuenca colombiana. *Rev. Cuad. del Caribe*, 2014.

[11] Timmermann, A. et al., El Niño: Southern oscillation complexity. *Nature*, **559**(7715), pp. 535–545, 2018.
[12] McMichael, A.J., Woodruff, R.E. & Hales, S., Climate change and human health: Present and future risks. *Lancet*, **367**(9513), pp. 859–869, 2006.
[13] Kim, J.-S., Zhou, W., Cheung, H.N. & Chow, C.H., Variability and risk analysis of Hong Kong air quality based on monsoon and El Niño conditions. *Adv. Atmos. Sci.*, **30**(2), pp. 280–290, 2013.
[14] Wie, J. & Moon, B.-K., ENSO-related PM_{10} variability on the Korean peninsula. *Atmos. Environ.*, **167**, pp. 426–433, 2017.
[15] Singh A. & Palazoglu, A., Climatic variability and its influence on ozone and PM pollution in six non-attainment regions in the United States. *Atmos. Environ.*, **51**, pp. 212–224, 2012.
[16] Singh A. & Palazoglu, A., A statistical framework to identify the influence of large-scale weather events on regional air pollution. *J. Appl. Meteorol. Climatol.,* **50**(12), pp. 2376–2393, 2011.
[17] Carslaw, D., The openair manual open-source tools for analysing air pollution data. *2015 David C. Carslaw*, London, p. 289, 2015.
[18] EPA, Method IO-3.5. Determination of metals in ambient particulate matter using inductively coupled plasma/mass spectrometry (ICP/MS). *Compendium of Methods for the Determination of Inorganic Compounds in Ambient Air*, 1st ed., Center for Environmental Research Information: Cincinnati, OH, pp. 1–35, 1999.
[19] C.P. Center, ENSO: Recent evolution, current status and predictions. 2015.
[20] Rojano, R.E., Manzano, C.A., Toro, R.A., Morales, R.G.E.S., Restrepo, G. & Leiva, M.A.G., Potential local and regional impacts of particulate matter emitted from one of the world's largest open-pit coal mines. *Air Qual. Atmos. Heal.*, **11**(5), pp. 601–610, 2018.
[21] Córdoba-Machado, S., Palomino-Lemus, R., Gámiz-Fortis, S.R., Castro-Diez, Y. & Esteban-Parra, M.J., Assessing the impact of El Niño modoki on seasonal precipitation in Colombia. *Glob. Planet. Change*, **124**, pp. 41–61, 2015.
[22] Poveda, G., Jaramillo, L. & Vallejo, L.F., Seasonal precipitation patterns along pathways of South American low-level jets and aerial rivers. *Water Resour. Res.*, **50**(1), pp. 98–118, 2014. DOI: 10.1002/2013WR014087.
[23] Tian, G., Qiao, Z. & Xu, X., Characteristics of particulate matter (PM_{10}) and its relationship with meteorological factors during 2001–2012 in Beijing. *Environ. Pollut.*, **192**, pp. 266–274, 2014.
[24] Unal, Y.S., Toros, H., Deniz, A. & Incecik, S., Influence of meteorological factors and emission sources on spatial and temporal variations of PM_{10} concentrations in Istanbul metropolitan area. *Atmos. Environ.*, **45**(31), pp. 5504–5513, 2011.
[25] Lee, J. & Kim, K.-Y., Analysis of source regions and meteorological factors for the variability of spring PM_{10} concentrations in Seoul, Korea. *Atmos. Environ.*, **175**, pp. 199–209, 2018.
[26] Boulanger, J.P., Leloup, J., Penalba, O., Rusticucci, M., Lafon, F. & Vargas, W., Observed precipitation in the Paraná-Plata hydrological basin: Long-term trends, extreme conditions and ENSO teleconnections. *Clim. Dyn.,* **24**(4), pp. 393–413, 2005.
[27] Power, S., Haylock, M., Colman, R. & Wang, X., The predictability of interdecadal changes in ENSO activity and ENSO teleconnections. *J. Clim.*, **19**(19), pp. 4755–4771, 2006.